

# Utilization of 3'-carboxy-containing tyrosine derivatives as a new class of phosphotyrosyl mimetics in the preparation of novel non-phosphorylated cyclic peptide inhibitors of the Grb2-SH2 domain

Yan-Li Song,<sup>a</sup> Jinzhi Tan,<sup>b</sup> Xiao-Min Luo<sup>b</sup> and Ya-Qiu Long<sup>\*a</sup>

Received 31st October 2005, Accepted 6th December 2005

First published as an Advance Article on the web 4th January 2006

DOI: 10.1039/b515432d

A new class of phosphotyrosyl (pTyr) mimetics, distinct from the conventional pTyr mimetic design of adding non-hydrolyzable acidic functionalities to the 4'-position of phenylalanine, was created by introducing carboxy-containing groups to the 3'-position of tyrosine. The effect of the chain length of the carboxy substituent was examined. Reported herein is the chiral pool synthesis of the new pTyr mimetics, and their first use in a novel non-phosphorylated Grb2-SH2 domain binding motif with the 5-amino-acid sequence Xx<sup>1</sup>-Leu-(3'-substituted-Tyr)-Ac6c-Asn. The highest affinity was exhibited by the 3-L-(2-carboxyethyl)tyrosine-containing sulfoxide-cyclized peptide **3c**, with an IC<sub>50</sub> = 1.1 μM, providing a promising new template for further development of potent Grb2-SH2 domain inhibitors with reduced charge and peptidic nature, but improved selectivity and bioavailability.

## Introduction

Growth factor receptor-bound protein 2 (Grb2) mediates intracellular signaling by its Src homology 2 (SH2) domain binding to phosphotyrosyl (pTyr) motifs on growth factor receptors, thereby leading to downstream activation of the mitogenic Ras pathways.<sup>1,2</sup> An aberrant Grb2-SH2 dependent Ras activation pathway has been shown to contribute to cellular processes important to cancer development and progression, including cell proliferation, apoptosis and metastasis.<sup>3,4</sup> Thus, compounds which selectively antagonize the SH2 domain of Grb2 should interrupt these signaling pathways and thus are attractive targets for drug therapy in oncology.<sup>5,6</sup>

Based on the unique structural feature that Grb2-SH2 domain preferentially associates with the peptide or protein ligands bearing the "pTyr-X-Asn" consensus sequence in a β-turn conformation,<sup>7</sup> many efforts in the development of Grb2-dependent signaling inhibitors have been focused on the creation of pTyr mimetics and pre-induced β-turn geometries.<sup>5</sup> These strategies are applicable to the phage library-based non-phosphorylated cyclic peptide antagonists of the Grb2-SH2 domain, which do not contain phosphotyrosine, yet can specifically bind to the target protein with high affinity (Fig. 1, lead compound **1**).<sup>8</sup> This new type of pTyr-independent Grb2-SH2 binding motif functions by a multi-point binding pattern involving well-defined side chains and specific conformations.<sup>9-13</sup> However, the phosphorylation of the Tyr residue within the consensus sequence of Tyr-Xx-Asn improved the binding affinity 100-fold with respect to G1TE.<sup>10</sup>

In combination with the recent finding that substitution at the 3'-position of the tyrosine greatly affects the activity of this non-phosphorylated peptide ligand of the Grb2-SH2 domain (Fig. 1, **2**),<sup>14</sup> we were intrigued to design a new class of pTyr mimetics by introducing one carboxyl group at the 3'-position of tyrosine and to incorporate it into a fully elaborated cyclic Grb2-SH2 domain-binding platform with reduced peptidic character (Fig. 1, **3**). This is a brand new strategy, distinct from previously reported pTyr mimetics in which the efforts were concentrated on the replacement of the 4'-phosphate of pTyr with phosphonate or dicarboxylate.<sup>15</sup> Although an earlier attempt to synthesize pTyr mimetics against the Grb2-SH2 domain by putting a carboxyl group at the 3'-position of the tyrosine proved unsuccessful when incorporated into an open-chain tripeptide platform,<sup>16</sup> we wanted to examine the new concept by trying various 3'-carboxyalkyl groups in the context of our novel non-phosphorylated Grb2-SH2 ligands. Reported herein is the chiral pool synthesis of an orthogonally protected L-3-(carboxyalkyl)tyrosine suitable for solid-phase peptide synthesis, and its first use in a new structural platform binding to the Grb2-SH2 domain, with only a 5-amino-acid sequence devoid of any pTyr or pTyr mimetics. The highest affinity was exhibited by the L-3-(2-carboxyethyl)tyrosine-containing sulfoxide-cyclized pentapeptide (**3c**) with an IC<sub>50</sub> of 1.1 μM, providing a new solution to the trade-off between the need for negatively charged pTyr mimetics for optimal affinity and the need to minimize charge to facilitate cell entry for all SH2 domain inhibitors.<sup>6</sup>

## Synthesis

Three new phosphotyrosyl mimetics bearing one carboxyl group with different chain lengths at the 3-position of L-tyrosine were synthesized in protected forms with *O*-Boc and *COO*-<sup>t</sup>Bu protection on the side chain and *N*-α-Fmoc protection on

<sup>a</sup>State Key Laboratory of Drug Research, Shanghai Institute of Materia Medica, Shanghai Institutes for Biological Sciences, Graduate School of the Chinese Academy of Sciences, CAS, 555 Zuchongzhi Road, Shanghai, 201203, China. E-mail: yqlong@mail.shnc.ac.cn; Fax: +86-21-50806876; Tel: +86-21-50806876

<sup>b</sup>Drug Discovery and Design Center, Shanghai Institute of Materia Medica, Shanghai Institutes for Biological Sciences, Graduate School of the Chinese Academy of Sciences, CAS, 555 Zuchongzhi Road, Shanghai, 201203, China

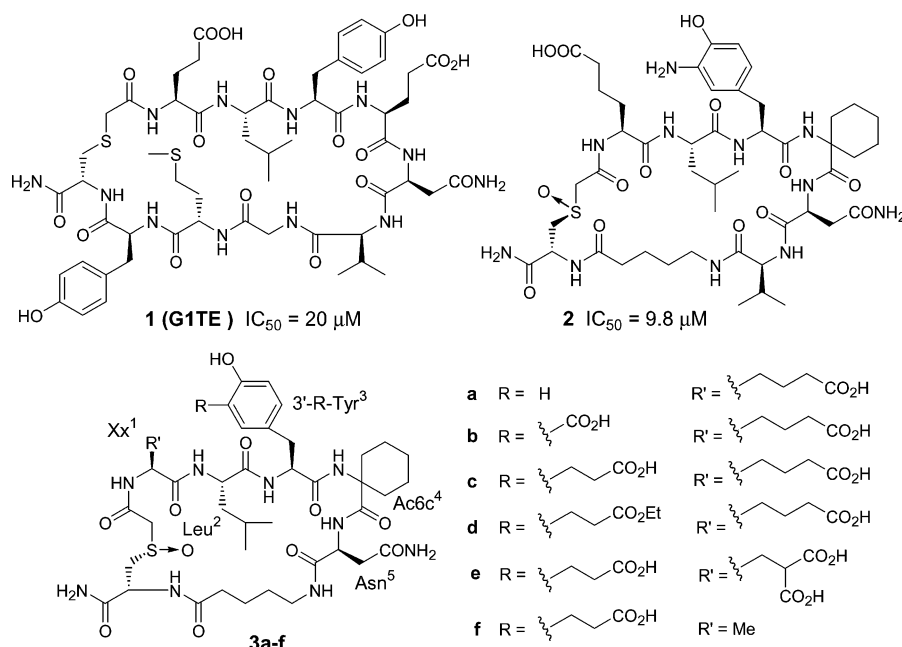
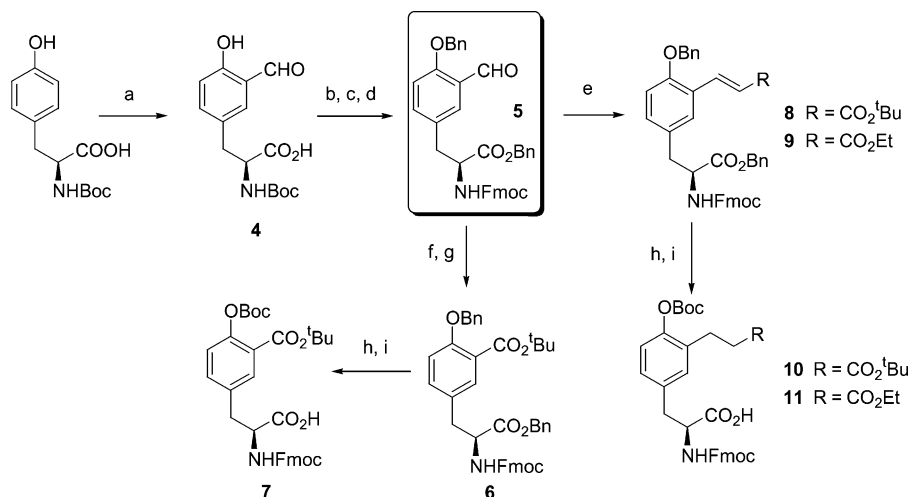


**Fig. 1** The structures of synthetic non-phosphorylated peptide ligands binding to the Grb2-SH2 domain.

the backbone, suitable for the solid-phase peptide synthesis. As outlined in Scheme 1, our synthesis begins with commercially available *N*-Boc-L-tyrosine. Formylation of the phenol using a modified Reimer–Tiemann process, namely treatment of the *N*-Boc-L-tyrosine with chloroform and solid sodium hydroxide in the presence of a small amount of water, gave the desired 3-formyl compound **4**.<sup>17</sup> Transformation of the *N*-Boc protection into *N*-Fmoc followed by the benzylation of the phenol group resulted in the key intermediate **5**. Compound **5** is a common intermediate for the synthesis of **7** through an oxidation pathway, and **10** and **11** through a Wittig sequence. The oxidation of the formyl group of **5** with  $\text{Ag}_2\text{O}$  under basic conditions and subsequent esterification of the resulting carboxylic acid with *tert*-butyl 2,2,2-

trichloroacetimidate afforded the fully protected compound **6**. Hydrogenation removed the benzyl protecting groups, and was followed by treatment with  $(\text{Boc})_2\text{O}$ , yielding the desired product **7**, orthogonally protected for solid-phase peptide synthesis. In the other route, treatment of **5** with different Wittig reagents provided compounds **8** and **9**. Hydrogenation followed by treatment with  $(\text{Boc})_2\text{O}$  furnished the desired compounds **10** and **11**, which were suitably protected for solid-phase peptide synthesis.

The 3'-(carboxyalkyl)tyrosine-containing cyclic peptides **3a–f** were synthesized manually using Fmoc-based SPS protocols on PAL amide resin.<sup>18</sup> Key intermediates included the *N*-terminally chloroacetylated derivative of the linear 5-mer precursor having cysteine at the *C*-terminal position with a  $\omega$ -aminovaleric



**Scheme 1** Synthetic route towards globally protected L-3-carboxyl-substituted tyrosines for solid-phase peptide synthesis. *Reagents and conditions:* (a) 6 eq. NaOH, 2 eq.  $\text{H}_2\text{O}$ ,  $\text{CHCl}_3$ , reflux; (b) 20% TFA in 10 mL DCM, rt; (c) 1.2 eq. FmocOSu, 10%  $\text{Na}_2\text{CO}_3$ , 0 °C to rt; (d) 2.5 eq.  $\text{BnBr}$ , 2.5 eq.  $\text{K}_2\text{CO}_3$ ,  $^t\text{Bu}_4\text{NI}$ , DMF, rt; (e) 1.0 eq.  $\text{Ph}_3\text{PCHR}$ , DCM, rt; (f) 2.0 eq.  $\text{Ag}_2\text{O}$ , 5% NaOH; (g) 3 eq. *tert*-butyl 2,2,2-trichloroacetimidate, THF–hexane; (h)  $\text{H}_2$ , 10% Pd/C, EtOH, rt; (i) 2.0 eq.  $(\text{Boc})_2\text{O}$ , cat. DMAP, 2.0 eq.  $\text{Et}_3\text{N}$ , DCM, rt.

acid linker in between. Peptide cyclization was achieved by intramolecular nucleophilic displacement of the chloro group by the cysteine side-chain thiol functionality. The oxidation of the thioether linkage into sulfoxide was readily achieved using 5% aqueous  $\text{H}_2\text{O}_2$ . The resulting sulfoxide diastereoisomers were easily separated by RP-HPLC. The stereochemistry of the sulfoxide diastereoisomers was identified by CD spectroscopy. The faster-eluting sulfoxide was the *R*-diastereomer, and the slower-eluting sulfoxide the *S*-diastereomer.<sup>19</sup> All final products were purified by RP-HPLC, their identities assessed by mass spectroscopy, and their purity checked by analytical HPLC.

## Results and discussion

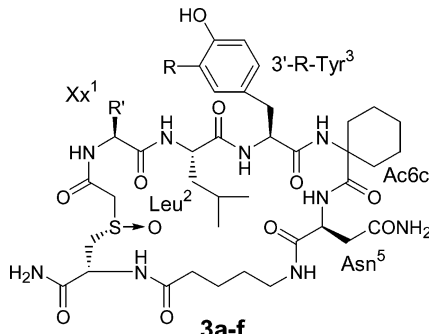
Because of the important role of SH2 domains in signal transduction pathways, SH2-mediated protein–protein interactions are attractive therapeutic targets. However, a major difficulty in designing SH2 domain-binding antagonists is the concentrated negative charge of SH2 ligands (from phosphate and acidic side chains), which would confer poor cellular activity and selectivity.<sup>20</sup> Therefore, phosphotyrosyl mimetics that retain high binding affinity yet exhibit reduced net anionic charge is recognized and pursued as an effective strategy to tackle such problems.

Our starting point is a phage library derived non-phosphorylated thioether-bridged cyclic decapeptide ligand (Fig. 1, **1**).<sup>8</sup> In order to reduce the peptidic character, a new cyclic Grb2–SH2 domain-binding platform was developed in which the peptide chain was shortened to a 5-amino-acid sequence, and a turn-inducing amino acid, namely  $\alpha$ -aminocyclohexanecarboxylic acid (Ac6c), incorporated at position 4. The cyclization linkage adopted was the favored (*R*)-configured sulfoxide<sup>12</sup> in the context of non-phosphorylated cyclic Grb2–SH2 binding peptides. The resulting (*R*)-sulfoxide-cyclized pentapeptide **3a** displayed moderate inhibitory activity ( $\text{IC}_{50} = 77 \mu\text{M}$ ), serving as the structural platform for the incorporation of new pTyr mimetics bearing one carboxy group at the 3-position of tyrosine (Table 1).

pTyr mimetics containing phosphonate- and carboxylate-based structures have been reported in the literature.<sup>14</sup> To date, monoacidic phosphoryl mimetics have tended to exhibit less affinity than diacidic mimetics, due in part to the presence of two highly conserved positively charged Arg residues within the SH2 domain pTyr binding pocket. In particular, the monocarboxy series, *e.g.*, carboxymethylphenylalanine, while useful in decreasing the net negative charge relative to pTyr, decreased affinity almost 100-fold, underscoring the importance of two negative charges for molecular recognition by SH2 domains in the context of regular linear phosphopeptides.<sup>21</sup>

Unlike the phosphopeptide ligands of Grb2–SH2 in which phosphotyrosine is a major contributor to the binding, our phage library based non-phosphorylated cyclic peptide antagonist requires essentially all amino acids (except Gly<sup>7</sup>), as well as the constrained conformation, to retain high affinity binding with the Grb2–SH2 domain.<sup>11–13</sup> It is hoped that this multipoint binding pattern and conformational constraint may allow improved interaction with the Grb2–SH2 domain by the incorporation of 3-carboxytyrosine-based pTyr mimetics with monocarboxy functionality.

**Table 1** The inhibitory activity of 3'-(carboxyalkyl)tyrosine-containing sulfoxide-bridged pentapeptides<sup>a</sup>



Compd.	R	R'	$\text{IC}_{50}/\mu\text{M}^b$
<b>3a</b>	-H	$-\text{CH}_2(\text{CH}_2)_2\text{COOH}$	$77.0 \pm 13.0$
<b>3b</b>	-COOH	$-\text{CH}_2(\text{CH}_2)_2\text{COOH}$	$16.5 \pm 3.5$
<b>3c</b>	$-\text{CH}_2\text{CH}_2\text{COOH}$	$-\text{CH}_2(\text{CH}_2)_2\text{COOH}$	$1.1 \pm 0.1$
<b>3d</b>	$-\text{CH}_2\text{CH}_2\text{CO}_2\text{Et}$	$-\text{CH}_2(\text{CH}_2)_2\text{COOH}$	$40.0 \pm 7.0$
<b>3e</b>	$-\text{CH}_2\text{CH}_2\text{COOH}$	$-\text{CH}_2\text{CH}(\text{COOH})_2$	$44.5 \pm 16.5$
<b>3f</b>	$-\text{CH}_2\text{CH}_2\text{COOH}$	$-\text{CH}_3$	$14.0 \pm 2.0$

<sup>a</sup> The competitive binding affinity of ligands for the Grb2–SH2 domain protein was assessed using Biacore surface plasmon resonance (SPR) methods.  $\text{IC}_{50}$  values were determined by mixing the inhibitor with recombinant Grb2–SH2 protein and measuring the amount of binding at equilibrium to an immobilized SHC (pTyr-317) phosphopeptide in a manner similar to that reported previously.<sup>8</sup> <sup>b</sup> Values are calculated from at least two independent experiments, and are expressed as the concentration at which half-maximal competition was observed ( $\text{IC}_{50}$ ). Errors are expressed as the standard deviation.

To our delight, when Tyr<sup>3</sup> was replaced with 3-carboxytyrosine, the resulting peptide **3b** exhibited a 4.6-fold increase in the binding potency ( $\text{IC}_{50} = 16.5 \pm 3.5 \mu\text{M}$ ) relative to the parent compound **3a** (Table 1). The chain length of the monocarboxy-based substituent at the 3'-position of Tyr was found to play an important role in the Grb2–SH2 binding. Just extending the side-chain of the 3'-carboxy substituent with two methylene units, *i.e.* substitution of Tyr with 3'-(2-carboxyethyl)tyrosine, provided peptide **3c**, displaying a 14-fold and 70-fold enhancement in Grb2–SH2 domain antagonist potency ( $\text{IC}_{50} = 1.1 \pm 0.1 \mu\text{M}$ ) relative to its zero-linker congener **3b** and the parent compound **3a**, respectively (Table 1). The gain in activity caused by the introduction of the linker might be attributed to an optimal positioning of the carboxyl group into the binding pocket by the flexible long side-chain. As expected, the loss of the free carboxylic acid by formation of the ethyl ester **3d**, *i.e.* replacement of Tyr<sup>3</sup> with L-3-(2-(ethylcarboxy)ethyl)tyrosine resulted in a marked decrease in the activity ( $\text{IC}_{50} = 40.0 \pm 7.0 \mu\text{M}$ ) (Table 1), suggesting that the acidic groups at the side chain of the tyrosine provide the key ionic interactions with the charged guanidine groups of the Arg67 ( $\alpha$ A-helix) and Arg86 ( $\beta$ C-strand) residues within the pTyr binding pocket. However, the ethyl ester **3d** could be used as a potential prodrug of **3c** in the future.

A previous SAR study has disclosed that the Glu<sup>1</sup> side chain in G1TE (**1**) compensates for the absence of Tyr<sup>3</sup> phosphorylation in securing effective binding to the Grb2–SH2 domain.<sup>9</sup> Thus, replacement of Glu<sup>1</sup> with  $\gamma$ -carboxyglutamic acid (Gla) prominently improves binding affinity.<sup>11–14</sup> However, in our case, in the presence of the L-3'-(2-carboxyethyl)tyrosine as a pTyr

mimetic, the introduction of Glu at position 1 (to give **3e**) adversely affects the binding, with a 40-fold decrease in the potency ( $IC_{50} = 44.5 \pm 16.5 \mu\text{M}$ ) compared to its precursor **3c** (Table 1). This negative result may indicate that the dicarboxyl side-chain of Glu<sup>1</sup> competes for the conformational space occupied by the carboxyl functionality of the pTyr mimetics, thus the crowded acidic groups interfere with the proper interactions with the binding pocket. This observation is similar to that found in pTyr-containing GITE analogs, in which the acidic Glu<sup>1</sup> is not favorable for binding.<sup>9</sup> Consistently, the replacement of Glu<sup>1</sup> with Ala<sup>1</sup> (to give **3e**), resulted in a 3-fold increase of the binding affinity ( $IC_{50} = 14.0 \pm 2.0 \mu\text{M}$ ) relative to the precursor **3d** (Table 1), while keeping a low net negative charge. These results are in agreement with the unique and important molecular mechanism disclosed by our previous SAR studies<sup>9–14</sup> for the non-phosphorylated cyclic Grb2–SH2 domain-binding motif with a 9-amino-acid sequence.

### Molecular modeling

The above observations can be nicely rationalized from the results of molecular modeling experiments. Based on the X-ray crystal structure of Grb2–SH2 domain having a bound cyclic phosphopeptide ligand,<sup>22</sup> we undertook molecular modeling studies to examine the interactions of peptides **3b**, **3c** and **3d** with the Grb2–SH2 domain protein, respectively. The automated molecular docking can produce several optional conformations of the inhibitors. The conformation corresponding to the lowest binding energy was selected as the possible binding conformation, as shown in Fig. 2.

In the final models (Fig. 2), it is evident that the carboxyl group introduced at the 3'-position of tyrosine makes key hydrogen bonding interactions with residues Arg67, Arg86 and Ser96 within the pTyr binding pocket of the Grb2–SH2 protein. For peptide **3b**, the acidic hydroxyl group of the 3'-carboxytryrosine residue makes two H-bonding interactions with each guanidino group of Arg67 and Arg86, while the 4'-hydroxy group of the phenyl ring forms an H-bond with Ser90. As a comparison, when the side-chain of the 3'-carboxy substituent was extended by two CH<sub>2</sub> units, the L-3-(2-carboxyethyl)tyrosine-containing cyclic peptide **3c** gained two additional H-bonding interactions with the hydroxyl side chain of Ser96 and the guanidino side chain of Arg86, provided by the hydroxyl and the carbonyl group of the 3'-(2-carboxyethyl) side chain, respectively. However, for the L-3-(2-ethylcarboxyethyl)tyrosine-containing peptide **3d**, the loss of the free carboxyl acid group at the 3-position of Tyr resulted in a complete loss of the H-bonding interactions. The proposed binding mode is consistent with the activity data.

### Conclusions

In this study, we designed a new class of phosphotyrosyl mimetics by introducing carboxy-containing groups at the 3'-position of tyrosine for enhanced binding to Grb2–SH2 domain of non-phosphorylated cyclic peptide ligands with reduced charge. A chiral pool synthetic approach was developed to prepare orthogonally protected L-3-(carboxyalkyl)tyrosines suitable for solid-phase peptide synthesis. The incorporation of the new pTyr mimetics into a phage library-derived non-phosphorylated structural platform bearing only a 5-amino-acid sequence resulted in a significant

increase of the binding potency, which might be attributable to an enhanced electrostatic interaction originating from the 3'-carboxy group of the tyrosine. The highest affinity was exhibited by the L-3-(2-carboxyethyl)tyrosine-containing pentapeptide (**3c**) with an  $IC_{50} = 1.1 \mu\text{M}$ , providing a promising new strategy for the development of potent Grb2–SH2 domain inhibitors with reduced charge and peptidic nature. This strategy may potentially find value in SH2 domain systems other than Grb2, where pTyr serves as a critical recognition determinant for effective binding.

## Experimental

### Binding affinity measurement of peptides to Grb2–SH2 domain using Surface Plasmon Resonance (SPR)

The competitive binding affinity of ligands for the Grb2–SH2 protein was assessed using Biacore SPR methods on a BIAcore 3000 instrument (Pharmacia Biosensor, Uppsala, Sweden).  $IC_{50}$  values were determined by mixing various concentrations of inhibitors with the recombinant GST–Grb2–SH2 domain protein and measuring the amount of binding at equilibrium to the immobilized SHC phosphopeptide (pTyr<sup>317</sup>), *i.e.* biotinyl-DDPS-pY-VNVQ, in a manner described previously.<sup>8</sup> Briefly, the biotinylated phosphopeptide was attached to a streptavidin-coated SA5 Biosensor chip, and the binding assays were conducted in pH 7.4 PBS buffer containing 0.01% P-20 surfactant (Pharmacia Biosensor).

### Molecular modeling

The advanced docking program Autodock 3.0.3<sup>24,25</sup> was used to automatically dock each of the three inhibitors to the binding pocket of the Grb2–SH2 protein. The crystal structure of Grb2–SH2 complexed with a cyclic phosphopeptide of cyclo(Ac-thiaLys-pTyr-Val-Asn-Val-Pro) (PDB entry code 1BM2)<sup>21</sup> was recovered from Brookhaven Protein Database (PDB). The missed side-chain atoms of Met55 were modeled by Sybyl 6.8 software.<sup>26</sup> The initial conformations of the three inhibitors were modeled based on the peptide in the crystal structure. The kinds of atomic charges were taken as Kollman-united-atom<sup>27</sup> for the protein and Gasteiger–Marsili<sup>28</sup> for the inhibitors.

The whole docking operation used in this study is as follows. First, the protein was checked for polar hydrogen and assigned for partial atomic charges, and then a PDBQ file was created, and the atomic solvation parameters assigned for the protein. Meanwhile, some of the torsion angles of the inhibitor that would be explored during the molecular docking stage were defined, allowing the conformation search for the ligand during the docking process. Second, a grid map with  $80 \times 80 \times 80$  points and a spacing of  $0.375 \text{ \AA}$  was calculated using the AutoGrid program,<sup>24</sup> to evaluate the binding energies between the inhibitor and the protein. Third, the Lamarckian genetic algorithm (LGA)<sup>24</sup> was applied to deal with the inhibitor–protein interaction. Some important parameters for LGA calculations were set as follows: an initial population of random individuals with a size of 500; a maximum number of  $1.5 \times 10^6$  energy evaluations; a maximum number of generations of  $5.0 \times 10^4$ . Default values were used for the other parameters. The energy minimization was performed by a Solis and Wets local search on a user-specified proportion of the



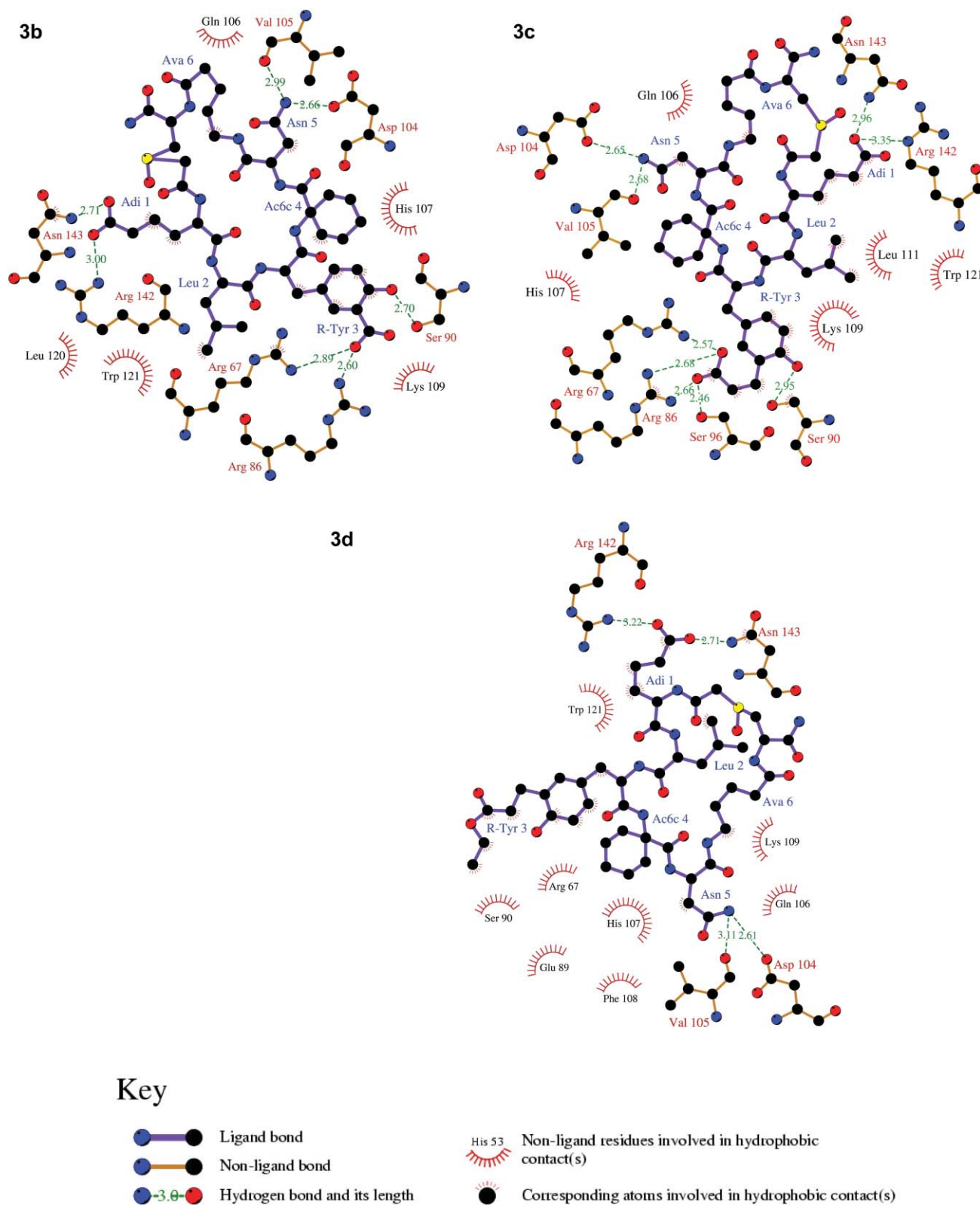


**Fig. 2** Two-dimensional representations of the interaction models of the 3-carboxytyrosine-containing cyclic peptide **3b**, the 3-(2-carboxyethyl)tyrosine-containing cyclic peptide **3c**, and the 3-(2-(ethylcarboxy)ethyl)tyrosine-containing cyclic peptide **3d** with the Grb2-SH2 protein. The images were generated with LIGPLOT program.<sup>23</sup>

population. Finally, the docked conformations of the inhibitor were selected according to the criterion of interaction energy combined with geometrical matching quality after a reasonable number of evaluations.

## Synthesis

The <sup>1</sup>H-NMR spectra were recorded on a Varian Mercury-400 MHz spectrometer. The data are reported in parts per million relative to TMS and referenced to the solvent in which they were run. Elemental analyses were obtained using a Vario EL spectrometer. Melting points (uncorrected) were determined on a Buchi-510 capillary apparatus. EI-MS spectra were obtained on a Finnigan MAT 95 mass spectrometer. ESI-MS spectra were obtained on a Finnigan LCQ Deca mass spectrometer. Specific rotations (uncorrected) were determined in a Perkin–Elmer 341 polarimeter. The solvent was removed by rotary evaporation under reduced pressure, and flash column chromatography was performed on silica gel H (10–40 μm). Anhydrous solvents were obtained by redistillation over sodium wire.

***N*-(1,1-Dimethylethoxy)carbonyl-3-(3-formyl-4-hydroxyphenyl)-L-alanine (4).** Powdered sodium hydroxide (1.71 g, 42.72 mmol) was added to a suspension of *N*-Boc-L-tyrosine (2 g, 7.12 mmol), water (0.256 mL, 14.13 mmol), and chloroform (30 mL). The mixture was refluxed for 4 h. Additional sodium hydroxide was added (0.84 g, 21.36 mmol) in two portions after 1 h and 1.5 h, respectively. The reaction was then diluted with water and ethyl acetate, and the aqueous layer was acidified to pH 1 with 1 N HCl and back-extracted with ethyl acetate. The organic extracts were washed with brine, dried over Na<sub>2</sub>SO<sub>4</sub>, and concentrated. Flash column chromatography (silica gel, 12 : 1 CHCl<sub>3</sub>–MeOH with 1% acetic acid as eluent) afforded the desired product **4** as a brown oil (720 mg, 33%). <sup>1</sup>H NMR (CDCl<sub>3</sub>, 400 MHz): δ 10.92 (1H, s), 9.84 (1H, s), 7.37 (d, 1H, *J* = 1.6 Hz), 7.33 (1H, d, *J* = 8.4 Hz), 6.74 (1H, d, *J* = 7.8 Hz), 5.28 (1H, bs), 4.96 (1H, m), 3.06–3.03 (2H, m), 1.40 (9H, s).

**3-(4-Benzoyloxy-3-formylphenyl)-2-(9H-fluoren-9-ylmethoxycarbonylamino)propionic acid benzyl ester (5).** Compound **4** (600 mg, 1.94 mmol) was dissolved in 20% TFA in DCM (10 mL), and the solution stirred at rt for 30 min. The solvent was then concentrated, and the residue dissolved in 10% Na<sub>2</sub>CO<sub>3</sub> (10 mL) and a solution of FmocOSu (786 mg, 2.3 mmol) in dioxane (10 mL) added dropwise, while stirring the mixture at rt overnight. Subsequently, the reaction mixture was poured into water and extracted with Et<sub>2</sub>O. The aqueous phase was acidified with 1 N HCl to pH 3, and the aqueous phase was back-extracted with EtOAc. The organic phase was dried over Na<sub>2</sub>SO<sub>4</sub>, and the solvent was removed *in vacuo*. The residue was dissolved in 10 mL DMF, and BnBr (0.56 mL, 4.64 mmol), K<sub>2</sub>CO<sub>3</sub> (640 mg, 4.64 mmol), and <sup>n</sup>Bu<sub>4</sub>NI (81 mg, 0.125 mmol) added. The mixture was stirred at rt overnight. Subsequently, the reaction mixture was poured into water and extracted with Et<sub>2</sub>O. The organic phase was dried over Na<sub>2</sub>SO<sub>4</sub>, and the solvent removed *in vacuo*. Flash column chromatography (silica gel, 1 : 4 EtOAc–PE as eluent) afforded the desired product **5** as a white foam (758 mg, 64%). <sup>1</sup>H NMR (CDCl<sub>3</sub>, 400 MHz): δ 10.49 (s, 1H), 7.77–7.26 (m, 19H), 7.16 (d, 1H, *J* = 8.4 Hz), 6.87 (d, 1H, *J* = 8.4 Hz), 5.36 (m, 1H), 5.18 (s, 2H), 5.14 (s, 2H), 4.70–4.64 (m, 1H), 4.45–4.11 (m, 3H), 3.13–3.04

(m, 2H). EI-MS: *m/z* 611 (M), 178 (100), 91 (24). HRMS: calcd for C<sub>33</sub>H<sub>39</sub>O<sub>6</sub>: 611.2308; found: 611.2315. [ $\alpha$ ]<sub>D</sub><sup>25</sup> = +3.2 (*c* = 1.7, CHCl<sub>3</sub>).

**2-Benzoyloxy-5-[2-benzoyloxycarbonyl-2-(9H-fluoren-9-ylmethoxycarbonylamino)ethyl]benzoic acid *tert*-butyl ester (6).** Compound **5** (220 mg, 0.36 mmol) was added to a stirred suspension of Ag<sub>2</sub>O (158 mg, 0.68 mmol) in 5% aq. NaOH (4 mL). After being stirred for 24 h, the suspension was filtered and the solid was washed with H<sub>2</sub>O. The filtrate was cooled to 0 °C, acidified with 1 N HCl, extracted with Et<sub>2</sub>O, and the extracts dried and concentrated. To the solution of the crude product and *tert*-butyl 2,2,2-trichloroacetimidate (398 mg, 1.35 mmol) in dry THF (10 mL), was added BF<sub>3</sub>·Et<sub>2</sub>O (50 μL). The solution was stirred at rt for 16 h, and then concentrated. The residue was diluted with saturated NaHCO<sub>3</sub> and ethyl acetate, and the aqueous layer back-extracted with ethyl acetate. The organic extracts were washed with H<sub>2</sub>O, brine, dried over Na<sub>2</sub>SO<sub>4</sub>, and concentrated. Flash column chromatography (silica gel, 6 : 1 PE–EtOAc) afforded the desired product **6** as a white solid (150 mg, 61%). <sup>1</sup>H NMR (CDCl<sub>3</sub>, 400 MHz): δ 7.76–7.26 (m, 19H), 7.16 (d, 1H, *J* = 8.4 Hz), 6.87 (d, 1H, *J* = 8.4 Hz), 5.36 (m, 1H), 5.18 (s, 2H), 5.14 (s, 2H), 4.72–4.10 (m, 4H), 3.13–3.04 (m, 2H), 1.50 (s, 9H).

**2-*tert*-Butoxycarbonyloxy-5-[2-carboxy-2-(9H-fluoren-9-ylmethoxycarbonylamino)ethyl]benzoic acid *tert*-butyl ester (7).** 10% Pd/C (10 mg) and **6** (315 mg, 0.46 mmol) was dissolved in dry EtOH (10 mL). The solution was stirred at rt overnight under H<sub>2</sub>. The Pd/C was filtered off and the filtrate concentrated *in vacuo* to afford a colorless oil (181 mg, 0.36 mmol). This residue, Boc<sub>2</sub>O (156 mg, 0.72 mmol), Et<sub>3</sub>N (20 mL), and cat. DMAP were dissolved in DCM (18 mL), and the solution stirred at rt for 2 h. The solvent was removed *in vacuo*. Flash column chromatography (silica gel, 1 : 4 EtOAc–PE as eluent) afforded the desired product **7** as a white foam (110 mg, 51%). <sup>1</sup>H NMR (CDCl<sub>3</sub>, 400 MHz): δ 7.76–7.26 (m, 8H), 7.18–7.02 (m, 3H), 5.59 (d, 1H, *J* = 8.0 Hz), 4.74–4.69 (m, 1H), 4.64–4.18 (m, 3H), 3.21–3.13 (m, 2H), 1.56 (s, 9H), 1.49 (s, 9H). ESI-MS: *m/z* 602 (M – H)<sup>–</sup>, 546 (M – <sup>t</sup>Bu), 530 (M – O<sup>t</sup>Bu). Anal. calcd for C<sub>34</sub>H<sub>37</sub>NO<sub>9</sub>: C, 67.65; H, 6.18; N, 2.32. Found: C, 67.76; H, 6.37; N, 2.06. [ $\alpha$ ]<sub>D</sub><sup>25</sup> = +19.8 (*c* = 0.5, CHCl<sub>3</sub>).

**3-{2-Benzoyloxy-5-[2-benzoyloxycarbonyl-2-(9H-fluoren-9-ylmethoxycarbonylamino)ethyl]phenyl}acrylic acid *tert*-butyl ester (8).** Ph<sub>3</sub>P=CHCO<sub>2</sub><sup>t</sup>Bu (273 mg, 0.80 mmol) was added to a solution of compound **5** (402 mg, 0.65 mmol) in DCM (15 mL), and the mixture stirred at rt for 10 h. The solvent was removed *in vacuo*. Flash column chromatography (silica gel, 1 : 6 EtOAc–PE as eluent) afforded the desired product **8** as a white foam (282 mg, 64%). <sup>1</sup>H NMR (CDCl<sub>3</sub>, 400 MHz): δ 7.69 (d, 1H, *J* = 16.0 Hz), 7.90–7.25 (m, 19H), 6.92 (dd, 1H, *J*<sub>1</sub> = 8.4 Hz, *J*<sub>2</sub> = 1.6 Hz), 6.76 (d, 1H, *J* = 8.4 Hz), 6.39 (d, 1H, *J* = 16.4 Hz), 5.31 (d, 1H, *J* = 8.4 Hz), 5.17 (d, 2H, *J* = 12.0 Hz), 5.09 (m, 1H), 4.71–4.67 (m, 1H), 4.46–4.41 (m, 3H), 3.08–3.05 (m, 2H), 1.49 (s, 9H). EI-MS: *m/z* (%) 709 (M<sup>+</sup>), 91 (100). HRMS: calcd for C<sub>43</sub>H<sub>39</sub>NO<sub>7</sub>: 709.3040; found: 709.3028. [ $\alpha$ ]<sub>D</sub><sup>25</sup> = –3.6 (*c* = 1.0, CHCl<sub>3</sub>).

**3-{2-Benzoyloxy-5-[2-benzoyloxycarbonyl-2-(9H-fluoren-9-ylmethoxycarbonylamino)ethyl]phenyl}acrylic acid ethyl ester (9).** Prepared from compound **5** (409 mg, 0.67 mmol) by a procedure similar to that used for **8**, to give **9** as a white foam (342 mg,

75%).  $^1\text{H}$  NMR ( $\text{CDCl}_3$ , 400 MHz):  $\delta$  7.98 (d, 1H,  $J = 16.4$  Hz), 7.76–7.23 (m, 19H), 6.92 (d, 1H,  $J = 8.4$  Hz), 6.76 (d, 1H,  $J = 8.4$  Hz), 6.47 (d, 1H,  $J = 16.4$  Hz), 5.31 (d, 1H,  $J = 8.4$  Hz), 5.19–5.10 (d, 2H,  $J = 12.4$  Hz), 5.10 (s, 2H), 4.71–4.17 (m, 4H), 4.23 (q, 2H,  $J = 7.2$  Hz), 3.08–3.05 (m, 2H), 1.31 (t, 3H,  $J = 7.2$  Hz). EI-MS: 681 ( $\text{M}^+$ ). HRMS: calcd for  $\text{C}_{43}\text{H}_{39}\text{NO}_7$ : 681.2727; found: 681.2735.  $[\alpha]_{\text{D}}^{25} = -2.5$  ( $c = 1.0$ ,  $\text{CHCl}_3$ ).

**3-{2-*tert*-Butoxycarbonyloxy-5-[2-carboxy-2-(9H-fluoren-9-ylmethoxycarbonylamino)ethyl]phenyl}acrylic acid *tert*-butyl ester (10).** Prepared from compound **8** (275 mg, 0.39 mmol) by a procedure similar to that used for **7**, to give **10** as a white foam (135 mg, 55%).  $^1\text{H}$  NMR ( $\text{CDCl}_3$ , 400 MHz):  $\delta$  7.79–7.28 (m, 8H), 7.03–6.97 (m, 3H), 5.41 (d, 1H,  $J = 8.4$  Hz), 4.65–4.60 (m, 1H), 4.43–4.18 (m, 3H), 3.10–3.07 (m, 2H), 2.81 (t, 2H,  $J = 8.0$  Hz), 2.48 (t, 2H,  $J = 8.0$  Hz), 1.53 (s, 9H), 1.44 (s, 9H). EI-MS:  $m/z$  (%) 530 ( $\text{M} - \text{CO}_2\text{tBu}$ ), 178 (100), 161 (12).  $[\alpha]_{\text{D}}^{25} = +13.6$  ( $c = 0.5$ ,  $\text{CHCl}_3$ ). Anal. calcd for  $\text{C}_{36}\text{H}_{41}\text{NO}_9$ : C, 68.45; H, 6.54; N, 2.22. Found: C, 68.76; H, 6.34; N, 1.79.

**3-[4-*tert*-Butoxycarbonyloxy-3-(2-(ethoxycarbonyl)ethyl)phenyl]-2-(9H-fluoren-9-ylmethoxycarbonylamino)propionic acid (11).** Prepared from compound **9** (241 mg, 0.35 mmol) by a procedure similar to that used for **7**, to give **11** as a white foam (109 mg, 51%).  $^1\text{H}$  NMR ( $\text{CDCl}_3$ , 400 MHz):  $\delta$  7.77–7.29 (m, 9H), 7.03–6.99 (m, 2H), 5.45 (d, 1H,  $J = 8.0$  Hz), 4.71–4.17 (m, 4H), 4.12 (q, 2H,  $J = 7.6$  Hz), 3.10–3.00 (m, 2H), 2.84 (t, 2H,  $J = 7.6$  Hz), 2.56 (t, 2H,  $J = 7.6$  Hz), 1.46 (s, 9H), 1.24 (t, 3H,  $J = 7.6$  Hz). EI-MS:  $m/z$  (%) 531 ( $\text{M} - \text{CO}_2\text{Et}$ ), 178 (100), 91 (45).  $[\alpha]_{\text{D}}^{25} = +15.6$  ( $c = 0.65$ ,  $\text{CHCl}_3$ ). Anal. calcd for  $\text{C}_{34}\text{H}_{37}\text{NO}_9$ : C, 67.65; H, 6.18; N, 2.32. Found: C, 67.95; H, 6.03; N, 1.88.

### General procedure for the synthesis of peptides 3a–f

All peptides were synthesized manually using standard solid-phase peptide chemistry with Fmoc-protected amino acids on Pal resin on a 0.1 mmol scale. HOBt/DIPCDI activation of  $\text{N}^{\alpha}$ -protected amino acids was employed for coupling, and 20% piperidine in DMF was used for Fmoc deprotection.  $\text{NH}_4\text{Ac}/\text{HOAc}$  buffer was used for backbone cyclization. TFA–TES– $\text{H}_2\text{O}$  (9.5 : 0.25 : 0.25) was used for the resin cleavage and side-chain deblocking. The oxidation of the thioether linkage into sulfoxide was accomplished using 5% aq.  $\text{H}_2\text{O}_2$ . The final product was purified by semi-preparative reverse-phase HPLC. HPLC conditions: Vydac C18 column (20  $\times$  250 mm). Solvent gradient system 1: **A**, 0.05% TFA in water, **B**, 0.05% TFA in 90% acetonitrile in water. Solvent gradient system 2: **A**, 0.05% TFA in water; **C**, 0.05% TFA in 90% methanol in water with gradient indicated below. Flow rate: 2.5 mL  $\text{min}^{-1}$ . UV detector: 225 nm. ESI-MS was performed on a Finnigan LCQ Deca mass spectrometer. The purity of products was characterized by analytical RP-HPLC using two solvent systems: method 1, gradient 10–70% **B** over 30 min; method 2, gradient 10–70% **C** over 30 min.

**Cyclo-[Ac-Adi-Leu-Tyr-Ac6c-Asn-Ava-Cys (O)-(R)]-amide (3a).** ESI-MS,  $m/z$ : calc. 932.4 ( $\text{M} - \text{H}$ ) $^-$ , found 932.3.  $t_{\text{R}} = 14.9$  min (10–70% of solvent **B** in 30 min, purity 98%);  $t_{\text{R}} = 20.9$  min (10–70% of solvent **C** in 30 min, purity 95%).

**Cyclo-[Ac-Adi-Leu-(3-CO<sub>2</sub>H-Tyr)-Ac6c-Asn-Ava-Cys (O)-(R)]-amide (3b).** ESI-MS,  $m/z$ : calc. 978.4 ( $\text{M} + \text{H}$ ) $^+$ , found 978.4.  $t_{\text{R}} = 15.1$  min (10–70% of solvent **B** in 30 min, purity 99%);  $t_{\text{R}} = 21.6$  min (10–70% of solvent **C** in 30 min, purity 96%).

**Cyclo-[Ac-Adi-Leu-(3-CH<sub>2</sub>CH<sub>2</sub>CO<sub>2</sub>H-Tyr)-Ac6c-Asn-Ava-Cys (O)-(R)]-amide (3c).** ESI-MS,  $m/z$ : calc. 1004.4 ( $\text{M} - \text{H}$ ) $^-$ , found 1004.7.  $t_{\text{R}} = 15.3$  min (10–70% of solvent **B** in 30 min, purity 98%);  $t_{\text{R}} = 21.4$  min (10–70% of solvent **C** in 30 min, purity 95%).

**Cyclo-[Ac-Adi-Leu-(3-CH<sub>2</sub>CH<sub>2</sub>CO<sub>2</sub>Et-Tyr)-Ac6c-Asn-Ava-Cys (O)-(R)]-amide (3d).** ESI-MS,  $m/z$ : calc. 1032.4 ( $\text{M} - \text{H}$ ) $^-$ , found 1032.4.  $t_{\text{R}} = 14.4$  min (10–70% of solvent **B** in 30 min, purity 98%);  $t_{\text{R}} = 20.3$  min (10–70% of solvent **C** in 30 min, purity 95%).  $^1\text{H}$ -NMR (600 MHz,  $\text{H}_2\text{O} + \text{D}_2\text{O}$ ):  $\delta$  8.70 (s, 1H), 8.39 (d, 1H,  $J = 8.4$  Hz), 8.28 (d, 1H,  $J = 6.0$  Hz), 8.11 (d, 1H,  $J = 7.2$  Hz), 7.69 (s, 1H), 7.62 (s, 1H), 7.54 (d, 1H,  $J = 6.0$  Hz), 7.50–7.48 (m, 2H), 7.15 (s, 1H), 6.86 (s, 1H), 6.74 (d, 1H,  $J = 6.6$  Hz), 6.83 (s, 1H), 6.51 (d, 1H,  $J = 6.6$  Hz), 4.39–4.36 (m, 2H), 4.09–4.01 (m, 3H), 3.60–3.46 (m, 3H), 3.28–3.05 (m, 2H), 3.03–2.71 (m, 10H), 2.28–2.10 (m, 6H), 1.67–1.63 (m, 1H), 1.53–1.44 (m, 4H), 1.47–1.37 (m, 10H), 1.36–1.16 (m, 6H), 0.76 (d, 3H,  $J = 6.6$  Hz), 0.68 (d, 1H,  $J = 6.6$  Hz).

**Cyclo-[Ac-Gla-Leu-(3-CH<sub>2</sub>CH<sub>2</sub>CO<sub>2</sub>H-Tyr)-Ac6c-Asn-Ava-Cys (O)-(R)]-amide (3e).** ESI-MS,  $m/z$ : calc. 1035.1 ( $\text{M} - \text{H}$ ) $^-$ , found 1035.4.  $t_{\text{R}} = 15.2$  min (10–70% of solvent **B** in 30 min, purity 96%);  $t_{\text{R}} = 22.1$  min (10–70% of solvent **C** in 30 min, purity 96%).

**Cyclo-[Ac-Ala-Leu-(3-CH<sub>2</sub>CH<sub>2</sub>CO<sub>2</sub>H-Tyr)-Ac6c-Asn-Ava-Cys (O)-(R)]-amide (3f).** ESI-MS,  $m/z$ : calc. 932.4 ( $\text{M} - \text{H}$ ) $^-$ , found 932.3.  $t_{\text{R}} = 16.7$  min (10–70% of solvent **B** in 30 min, purity 99%);  $t_{\text{R}} = 24.6$  min (10–70% of solvent **C** in 30 min, purity 95%).

### Acknowledgements

The Chinese Academy of Sciences (No. KSCX1-SW-11) and the Ministry of Science and Technology of China (No. 2004CB518903) are greatly appreciated for their financial support. The authors thank Professor Xu Shen and his colleagues of the DDDC at SIMM for their kind assistance when using their Biacore 3000 instrument.

### References

- 1 E. J. Lowenstein, R. J. Daly, W. L. Batzer, B. Margolis, R. Lanners, A. Ulrich, E. Y. Skolnick, D. Bar-Sagi and J. Schlessinger, *Cell*, 1992, **70**, 431–442.
- 2 T. Pawson and J. Schlessinger, *Curr. Biol.*, 1993, **3**, 434–442.
- 3 A. M. Tari, M. C. Hung, K. Li and G. Lopez-Berestein, *Oncogene*, 1999, **18**, 1325–1332.
- 4 J. V. Soriano, N. F. Liu, Y. Gao, Z.-J. Yao, T. Ishibashi, C. Underhill, T. R. Burke and D. P. Bottaro, *Mol. Cancer Ther.*, 2004, **3**, 1289–1299.
- 5 H. Fretz, P. Furet, C. Garcia-Echeverria, J. Rahuel and J. Schoepfer, *Curr. Pharm. Des.*, 2000, **6**, 1777–1796.
- 6 K. Machida and B. J. Mayer, *Biochim. Biophys. Acta*, 2005, **1747**, 1–25.
- 7 J. Rahuel, B. Gay, D. Erdmann, A. Strauss, C. Garcia-Echeverria, P. Furet, G. Caravatti, H. Fretz, J. Schoepfer and M. G. Grutter, *Nat. Struct. Biol.*, 1996, **3**, 586–589.
- 8 L. Oligino, F.-D. T. Lung, L. Sastry, J. Bigelow, T. Cao, M. Curran, T. R. Burke, S.-M. Wang, D. Krag, P. P. Roller and C. R. King, *J. Biol. Chem.*, 1997, **272**, 29046–29052.

- 9 Y.-Q. Long, J. H. Voigt, F.-D. T. Lung, C. R. King and P. P. Roller, *Bioorg. Med. Chem. Lett.*, 1999, **9**, 2267–2272.
- 10 Y.-Q. Long, Z.-J. Yao, J. H. Voigt, F.-D. T. Lung, J. H. Luo, T. R. Burke, C. R. King, D. Yang and P. P. Roller, *Biochem. Biophys. Res. Commun.*, 1999, **264**, 902–908.
- 11 F.-D. T. Lung, Y.-Q. Long, C. R. King, J. Varady, X.-W. Wu, S.-M. Wang and P. P. Roller, *J. Pept. Res.*, 2001, **57**, 447–454.
- 12 Y.-Q. Long, F.-D. Lung and P. P. Roller, *Bioorg. Med. Chem.*, 2003, **11**, 3929–3936.
- 13 Y.-Q. Long, R. Guo, J. H. Luo, D. Yang and P. P. Roller, *Biochem. Biophys. Res. Commun.*, 2003, **310**, 334–340.
- 14 Y.-L. Song, P. P. Roller and Y.-Q. Long, *Bioorg. Med. Chem. Lett.*, 2004, **14**, 3205–3208.
- 15 T. R. Burke, Jr. and K. Lee, *Acc. Chem. Res.*, 2003, **36**, 426–433.
- 16 Y. Gao, L. Wu, J. H. Luo, R. Guo, D. Yang, Z. Y. Zhang and T. R. Burke, *Bioorg. Med. Chem. Lett.*, 2000, **10**, 923–927.
- 17 M. E. Jung and T. I. Lazarova, *J. Org. Chem.*, 1997, **62**, 1553–1555.
- 18 E. Atherton and R. C. Sheppard, *Solid Phase Peptide Synthesis: A Practical Approach*, IRL, Oxford, 1989.
- 19 P. Li, M. Zhang, Y.-Q. Long, M. L. Peach, H. Liu, D. Yang, M. Nicklaus and P. P. Roller, *Bioorg. Med. Chem. Lett.*, 2003, **13**, 2173–2177.
- 20 W. C. Shakespeare, *Curr. Opin. Chem. Biol.*, 2001, **5**, 409–415.
- 21 S.-K. Kang, Z.-D. Shi, K. M. Worthy, L. K. Bindu, P. G. Dharmawardana, S. J. Choyke, D. P. Bottaro, R. J. Fisher and T. R. Burke, Jr., *J. Med. Chem.*, 2005, **48**, 3945–3948.
- 22 P. Ettmayer, D. France, J. Gounarides, M. Jarosinski, M.-S. Martin, J.-M. Rondeau, M. Sabio, S. Topiol, B. Weidmann, M. Zurini and K. W. Bair, *J. Med. Chem.*, 1999, **42**, 971–980.
- 23 A. C. Wallace, R. A. Laskowski and J. M. Thornton, *Protein Eng.*, 1995, **8**, 127–134.
- 24 G. M. Morris, D. S. Goodsell, R. S. Halliday, R. Huey, W. E. Hart, R. K. Belew and A. J. Olson, *J. Comput. Chem.*, 1998, **19**, 1639–1662.
- 25 G. M. Morris, D. S. Goodsell, R. Huey, W. E. Hart, R. S. Halliday, R. K. Belew and A. J. Olson, *Autodock (Version 3.0.3)*, Molecular Graphics Laboratory, Department of Molecular Biology, The Scripps Research Institute, La Jolla, CA, 1999.
- 26 *Sybyl (Version 6.8)*, Tripos Associates, St. Louis, MO, 2000.
- 27 S. J. Weiner, P. A. Kollman, D. A. Case, U. C. Singh, C. Ghio, G. Alagona, S. Profeta and P. Weiner, *J. Am. Chem. Soc.*, 1984, **106**, 765–784.
- 28 J. Gasteiger and M. Marsili, *Tetrahedron*, 1980, **36**, 3219–3228.